CSIRO PUBLISHING

Australian Journal of Physics

Volume 52, 1999

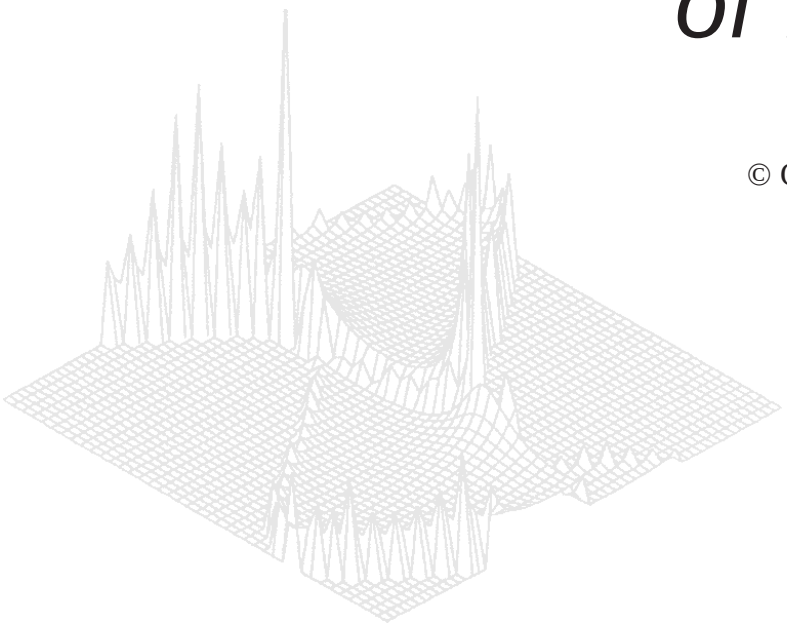

A journal for the publication of
original research in all branches of physics

www.publish.csiro.au/journals/ajp

All enquiries and manuscripts should be directed to
Australian Journal of Physics
CSIRO PUBLISHING
PO Box 1139 (150 Oxford St)
Collingwood Telephone: 61 3 9662 7626
Vic. 3066 Facsimile: 61 3 9662 7611
Australia Email: peter.robertson@publish.csiro.au

Published by **CSIRO** PUBLISHING
for CSIRO Australia and
the Australian Academy of Science

Aust. J. Phys., 1999, **52**, 1025–38

The Motion of Rapidly Rotating Curling Rocks

Mark R. A. Shegelski[A] *and Ross Niebergall*[B]

[A]Department of Physics, University of Northern British Columbia,
3333 University Way, Prince George, BC V2N 4Z9, Canada.
email: mras@unbc.ca

[B]Department of Mathematics and Computer Science,
University of Northern British Columbia,
3333 University Way, Prince George, BC V2N 4Z9, Canada.

Abstract

We present a physical model that accounts for the motion of rapidly rotating curling rocks. By rapidly rotating we mean that the rotational speed of the contact annulus of the rock about the centre of mass is large compared with the translational speed of the centre of mass. The principal features of the model are: (*i*) that the kinetic friction induces melting of the ice, with the consequence that there exists a thin film of liquid water lying between the contact annulus of the rock and the ice; (*ii*) that the curling rock drags some of the thin liquid film around the rock as it rotates, with the consequence that the relative velocity between the rock and the thin liquid film is significantly different to the relative velocity between the rock and the underlying solid ice surface. Since it is the former relative velocity which dictates the nature of the motion of the curling rock, our model predicts some interesting differences between the motions of slowly versus rapidly rotating rocks. Of principal note is that our model predicts, and observations confirm, that rapidly rotating curling rocks stop moving translationally well before rotational motion ceases. This is in sharp contrast to the usual case of slow rotation, where both rotational and translational motion cease at the same instant. We have verified this and other predictions of our model by careful comparison with the motion of actual curling rocks.

1. Introduction

The primary purpose of this paper is to present a physically plausible model that accounts both qualitatively and quantitatively for the motion of rapidly rotating curling rocks. This work is an extension of an earlier paper (Shegelski *et al*. 1996) in which we presented a model that accounted for the observed motion of slowly rotating curling rocks. We give here only a brief description of those aspects of curling that the reader will need to know in order to appreciate the physics addressed in this paper. More details are given in our previous paper (Shegelski *et al*. 1996).

Curling rocks have a small contact area with the ice: the bottom of the rock is hollowed and curved. Only a thin annulus of radius $r \approx 6{\cdot}25$ cm and width $\Delta r \approx 3$ to 5 mm makes contact with the ice. Moreover, the sheet of ice is *not* flat. Instead, the surface of curling ice consists of many rounded protrusions with accompanying hollows, and is referred to as 'pebbled ice'. One consequence of

 10.1071/PH98064 0004-9506/99/061025$05.00

the nature of the ice surface is that only a fraction of the annulus of the curling rock makes contact with the ice. This results in higher pressure exerted on the ice by the rock. The pressure results in melting of the ice as the rock passes over it. (This melting is *not* due to the pressure *directly*, but instead occurs because of the relative motion between the rock and the ice.)

We begin by explaining our hypotheses and assumptions. We then present the equations that describe the motion of a rapidly rotating curling rock. By rapid rotation we mean that the speed with which the contact annulus rotates about the centre of mass is large compared with the translational speed of the centre of mass. The equations are solved numerically to obtain the development in time of the rock's translational and rotational speeds. The results are compared with observed motions.

2. Theory of the Motion of Rapidly Rotating Curling Rocks

Consider first the case of no translational motion. Once the rock has been released and is rotating, the relative motion between the contact annulus and the ice will induce kinetic melting of the ice. The thin liquid film will then be subjected to the adhesive force between granite and water. Some of the liquid will thus be accelerated and will tend to be drawn around the contact ring. As the rock rotates, the liquid film beneath it will flow/rotate in the same sense as the rock. The liquid closest to the rock will rotate the fastest, whereas the liquid nearest the ice will exhibit essentially no rotation. The main consequence of this is that the velocity of the rock relative to the liquid film immediately beneath it will be considerably smaller than the velocity of the rock relative to the underlying solid ice surface. Denoting the velocity of a small portion of the contact annulus of the rock, relative to the solid ice surface, by $\vec{v}_{r/s} \equiv \vec{v}_s$, and the velocity of the portion of the rock's contact annulus relative to the adjacent liquid film by $\vec{v}_{r/liq} \equiv \vec{v}_{liq}$, we have $\vec{v}_{r/liq} = \epsilon \vec{v}_{r/s}$, or $\vec{v}_{liq} = \epsilon \vec{v}_s$, with $0 < \epsilon < 1$. (Note that $\vec{v}_{liq} = \epsilon \vec{v}_s$ only when there is no translational motion; see below.)

Consider next the case where the rock rotates rapidly and moves arbitrarily slowly translationally (i.e. $r\omega_0 > > v_0$, with v_0 arbitrarily small). The ideas of the above paragraph still apply, except we need to include the translational motion.

Consider a given portion of the contact annulus of the rock. This portion will have a velocity $\vec{v}_s$ relative to the solid ice surface. Given that the rock is rotating rapidly and moving translationally very slowly, the contact annulus will still tend to drag some of the liquid film around it. We see that the adhesion of the liquid film will be such that the liquid will be dragged around primarily *tangent* to the contact annulus, and almost not at all *perpendicular* to the contact annulus. The consequence of this is that the velocity $\vec{v}_{liq}$ of the portion of the contact annulus relative to the adjacent liquid film will be given by

$$\vec{v}_{liq} = \epsilon \vec{v}_t + \vec{v}_r \,, \tag{1}$$

where $\vec{v}_t$ and $\vec{v}_r$ are the *tangential* and *radial* components of the velocity relative to the solid ice surface and $0 < \epsilon < 1$; see Fig. 1.

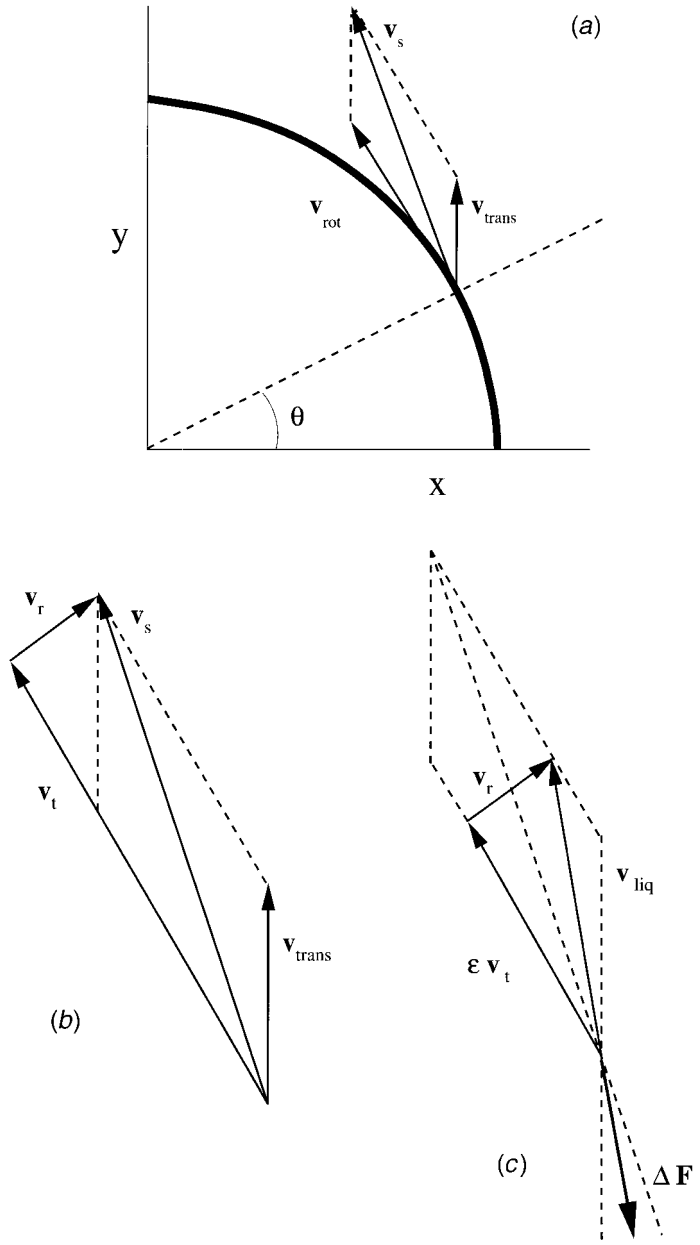

Fig. 1. (*a*) The contributions $\vec{v}_{trans}$ and $\vec{v}_{rot}$ (with $v_{rot} = r\omega$) to the net velocity $\vec{v}_s \equiv \vec{v}_s(\theta)$, relative to the ice, of a portion of the contact annulus located at an angle θ relative to the x-axis: $\vec{v}_s = \vec{v}_{trans} + \vec{v}_{rot}$. (*b*) The tangential and radial components of $\vec{v}_s$, $\vec{v}_t$ and $\vec{v}_r$: $\vec{v}_s = \vec{v}_t + \vec{v}_r$. (*c*) The net velocity $\vec{v}_{liq} \equiv \vec{v}_{liq}(\theta)$, *relative to the underlying thin liquid film*: $\vec{v}_{liq} = \epsilon\vec{v}_t + \vec{v}_r$. The figures shown are for a portion located in the first quadrant; similar figures are readily constructed for the other three quadrants. The angle θ in each case is from the x-axis toward the y-axis. Note that the parallelogram in part (*c*) is the same as the one in part (*a*). Also note that the force $\Delta\vec{F}$ exerted on the portion is in the direction *opposite to* $\vec{v}_{liq}$, and that this direction is *different to the direction opposite to* $\vec{v}_s$.

We emphasise that $\vec{v}_{liq}$ and $\vec{v}_s$ are *not* in the same direction! We have

$$\vec{v}_s = \vec{v}_{trans} + \vec{v}_{rot}\,, \tag{2}$$

where $\vec{v}_{trans}$ is the translational velocity of the centre of mass relative to the ice, and $\vec{v}_{rot}$ is the 'rotational' velocity of a given portion of the contact annulus relative to the centre of mass, as shown in Fig. 1. In order to convey ideas as clearly as possible, we next consider the extreme limit $\epsilon \to 0$. In the $\epsilon \to 0$ limit, $\vec{v}_{liq}$ would be radially outward for the front half of the rock, and radially inward for the back half. In this extreme, there would be no torque to slow the rotation of the rock, but there would still be a net force in the direction opposite to the velocity of the centre of mass, and thus the rock would exhibit decreasing translational motion until it came to a stop.

In the case that $0 < \epsilon < 1$ with ϵ small enough, we again have that the direction of the force acting on a given portion of the contact annulus is opposite in direction to $\vec{v}_{liq}$, and *not* $\vec{v}_s$, as is clear in Fig. 1. Consequently, the torque will once again be diminished, and the rotational motion will continue for a longer time than the translational motion.

We may regard equation (1) for $\vec{v}_{liq}$ as a hypothesis. We will see that the predictions of equation (1) are confirmed. In particular, that translational motion ceases well before rotational motion for rapidly rotating curling rocks is a prediction of equation (1) that is confirmed by observation of actual curling rocks. Such agreements will then elevate our proposal to that of a model. We emphasise that the alternative proposal that $\vec{v}_{liq} = \epsilon\vec{v}_s$ has the consequence that rotational and translational motion cease simultaneously, contrary to what is observed, thus rendering this alternative proposal incorrect.

In summary, our model predicts that the motion of the rock over the ice gives kinetic melting and a thin liquid film; the thin film is dragged around the rock by adhesion, with the result that, in the case of rapid rotation, the forces on the contact points are *not* opposite to the directions of motion of the contact points *relative to the solid ice surface*. The consequence is that translational motion ceases before rotational motion.

We tested this prediction by projecting curling rocks with large initial angular speeds and small initial translational speeds. We observed that the duration of translational motion was shorter than that of rotational motion, and found that the larger the ratio $r\omega_0/v_0$, the greater the difference in the times taken for rotation to stop and for translation to stop.

3. Equations of Motion of a Rapidly Rotating Curling Rock

We next give the equations which determine the motion of a rapidly rotating curling rock. This is a straightforward exercise in determining the net force and torque exerted on the rock by the thin film adjacent to the contact annulus.

We find that the lateral motion of the rock is, both theoretically and observationally, negligible: a rapidly rotating curling rock exhibits essentially no curl. Consequently, we focus on only the time-dependence of the translational speed $v(t)$ and rotational speed $\omega(t)$.

We choose coordinate axes as follows. The y-axis is in the direction of the initial velocity of the rock, and the x-axis is perpendicular to the initial velocity.

We break up the rock into four quadrants, and define θ as the angle from the x-axis toward the y-axis with $0 \leq \theta \leq \pi/2$.

We take the friction exerted on a small section of the annulus of the rock to be in the direction opposite to the velocity $\vec{v}_{liq}(\theta)$ of the point relative to the adjacent liquid film. The magnitude of the friction is $\Delta F = \mu M g(\Delta\theta/2\pi)$, where μ is the coefficient of kinetic friction, M is the mass of the rock, and g is the acceleration due to gravity. (In the case of a curling rock, the nonuniformity in the normal force around the rock is negligible in our model; the nonuniformity is a consequence of the acceleration due to friction.)

In order to simplify the treatment of rapid rotation, we take the magnitude ΔF of the friction to be approximately constant; i.e. we take μ to be constant. In our previous work, we took the magnitude of the wet friction to increase with velocity, in analogy with the increased drag on an object moving in a fluid. In the case of rapid rotation, this is not the most appropriate approach. Our reasoning is as follows.

We expect that both ϵ and μ will exhibit complicated time-dependencies. This expectation will be supported upon comparing our model with detailed observations (see Fig. 5 below). However, it is beyond the scope of this work to obtain and employ a first-principles derivation of the time-dependent forms of $\epsilon(t)$ and $\mu(t)$. Our focus will be, instead, to take ϵ and μ as effective values which reproduce the principal features of the overall motion. We will see below that this is indeed a fruitful approach, and we will comment on this later in the paper.

By considering each quadrant of the rock separately, the following equations for the net force and the net torque on the rock are readily obtained. We have

$$F = -\frac{1}{\pi}\mu M g \int_0^{\pi/2} d\theta \Bigg[\cos\left(\theta + \tan^{-1}\left[\frac{v\sin\theta}{\epsilon(r\omega + v\cos\theta)}\right]\right) - \cos\left(\theta - \tan^{-1}\left[\frac{v\sin\theta}{\epsilon(r\omega - v\cos\theta)}\right]\right)\Bigg]. \tag{3}$$

The equation for the torque is

$$\tau = -\frac{1}{\pi} r\mu M g \int_0^{\pi/2} d\theta \Bigg[\cos\left(\tan^{-1}\left[\frac{v\sin\theta}{\epsilon(r\omega + v\cos\theta)}\right]\right) + \cos\left(\tan^{-1}\left[\frac{v\sin\theta}{\epsilon(r\omega - v\cos\theta)}\right]\right)\Bigg]. \tag{4}$$

In these equations $v(t) \equiv v \equiv v_{trans}$ is the instantaneous speed of the centre of mass of the rock; $\omega(t) \equiv \omega$ is the instantaneous angular speed of the rock; and θ in each quadrant is measured from the x-axis toward the y-axis, as shown in Fig. 1.

Fig. 1 is presented to assist in understanding the above equations. Fig. 1*a* shows the contributions $\vec{v}_{trans}$ and $\vec{v}_{rot}$ (with $v_{rot} = r\omega$) to the net velocity $\vec{v}_s \equiv \vec{v}_s(\theta)$, relative to the ice, of a portion of the contact annulus located at angle θ; recall that $\vec{v}_s = \vec{v}_{trans} + \vec{v}_{rot}$, and recall that the velocity of the centre of mass of the rock relative to the ice is simply $\vec{v}_{trans}$. Fig. 1*b* shows $\vec{v}_s$ in terms of its tangential component $\vec{v}_t$ and its radial component $\vec{v}_r$: $\vec{v}_s = \vec{v}_t + \vec{v}_r$. Note that $v_t = r\omega \pm v\cos\theta$ and $v_r = v\sin\theta$. Fig. 1*c* shows the velocity, $\vec{v}_{liq}$, of the portion of the contact annulus at angle θ, relative to the underlying thin liquid film: $\vec{v}_{liq} = \epsilon\vec{v}_t + \vec{v}_r$. Also shown in this figure is the force $\Delta\vec{F}$ exerted on the portion of the contact annulus. We emphasise that $\Delta\vec{F}$ is in the direction *opposite to* $\vec{v}_{liq}$, and that this is *not the same as the direction opposite to* $\vec{v}_s$, as is manifest from Fig. 1.

Similar figures are readily constructed for the other three quadrants of the rock. The equations above include the contributions from each of the four quadrants.

The velocity of the rock at any time t is readily obtained numerically from the above equations along with $\vec{F} = Md\vec{v}/dt$, and initial conditions:

$$v(t) = v_0 + \int_0^t dt' a(t')\,, \tag{5}$$

where $a = F/M$ is simply the acceleration of the centre of mass. The angular speed ω is given by

$$\omega(t) = \omega_0 + \int_0^t dt' \alpha(t')\,, \tag{6}$$

where $\tau = \frac{1}{2}MR^2\alpha$ determines the time development of the angular acceleration α of the rock; M is the mass of the rock and R is the radius of the rock. Note that the radius of the contact annulus is smaller than the radius of the rock: $r \approx 6{\cdot}25$ cm; $R \approx 14{\cdot}0$ cm. (In our previous paper we used a different value for r. With the value cited in this paper, the results and conclusions of our previous work are unchanged.)

The coefficient of friction μ may be estimated by observation of rapidly rotating rocks. This would leave ϵ as the single parameter in the problem. Alternatively, if an estimate of ϵ is made, μ may be regarded as the single parameter.

Equations (3)–(6) are readily solved to leading order in either of the two extremes $\epsilon r\omega \gg v$ or $r\omega \ll v$. [Equations (3) and (4) for the force and torque, as given above, are for the case $r\omega > v$. The corresponding expressions for $r\omega < v$ are slightly different (see Shegelski *et al.* 1996); attention must be paid to these differences when considering all ranges of the ratio $r\omega/v$.] The results for the two limits are as follows:

For $\epsilon r\omega \gg v$:

$$v(t) = v_0\left(1 - \frac{t}{t_0}\right)^{\phi_1}, \quad \omega(t) = \omega_0\left(1 - \frac{t}{t_0}\right), \tag{7}$$

with

$$t_0 = \frac{R^2}{2r^2}\frac{r\omega_0}{\mu g}, \quad \phi_1 = \frac{R^2}{4\epsilon r^2}\,; \tag{8}$$

for $r\omega \ll v$:

$$v(t) = v_0\left(1 - \frac{t}{t_0}\right), \quad \omega(t) = \omega_0\left(1 - \frac{t}{t_0}\right)^{\phi_2}, \tag{9}$$

with

$$t_0 = \frac{v_0}{\mu g I_0(\epsilon)}, \quad \phi_2 = \frac{2r^2 I_1(\epsilon)}{R^2 I_0(\epsilon)}\,, \tag{10}$$

where

$$I_0(\epsilon) = \frac{2}{\pi}\int_0^{\pi/2} d\theta \cos\left(\tan^{-1}\left[\frac{1}{\epsilon}\tan\theta\right] - \theta\right) \tag{11}$$

and

$$\begin{aligned} I_1(\epsilon) &= \frac{2\epsilon}{\pi}\int_0^{\pi/2} d\theta \frac{\sin\theta}{\sin^2\theta + \epsilon^2\cos^2\theta}\sin\left(\tan^{-1}\left[\frac{1}{\epsilon}\tan\theta\right]\right) \\ &= \frac{2\epsilon}{\pi}\int_0^{\pi/2} d\theta \frac{\sin^2\theta}{\left[\sin^2\theta + \epsilon^2\cos^2\theta\right]^{\frac{3}{2}}}. \end{aligned} \tag{12}$$

In these equations, t_0 represents the *approximate* stopping time. It is very important to recognise that these asymptotic forms are good approximations provided either $r\omega \ll v$ or $\epsilon r\omega \gg v$, as the case may be, and that these approximations may well break down as $t \to t_0$.

The exact numerical results shown in the figures in the next section will be compared to these asymptotic forms. We will see that the approximations are very good, and break down only toward the end of the motion of the rock. We comment on this more fully later.

4. Results

We have examined several numerical runs for a variety of choices of v_0, ω_0 and ϵ. In Figs 2–4 we show curves for $v(t)/v_0$ and $\omega(t)/\omega_0$ as functions of time t for selected values of ϵ and the ratio $s_0 \equiv v_0/r\omega_0$. We compare the (exact) numerical results to the leading asymptotic analytical expressions whenever the motion is in one of the two extremes $\epsilon r\omega \gg v$ [part (a) in Figs 2 and 3] or $r\omega \ll v$ (Fig. 4). In Figs 2–4, the values of ϵ are $0{\cdot}1$, $0{\cdot}4$ and $1{\cdot}0$. In part (a) in Figs 2 and 3 we have $s_0 = 0{\cdot}1$, while in part (b) $s_0 = 1$. In Fig. 4, we have $s_0 = 20$.

The insight gained from Figs 2 and 3 will be used for comparison of the model with observations of the motions of actual, rapidly rotating curling rocks. In all these figures, the same value for μ was used; we chose $\mu = 0{\cdot}0125$ as this is a typical value for curling rocks (Shegelski *et al.* 1996).

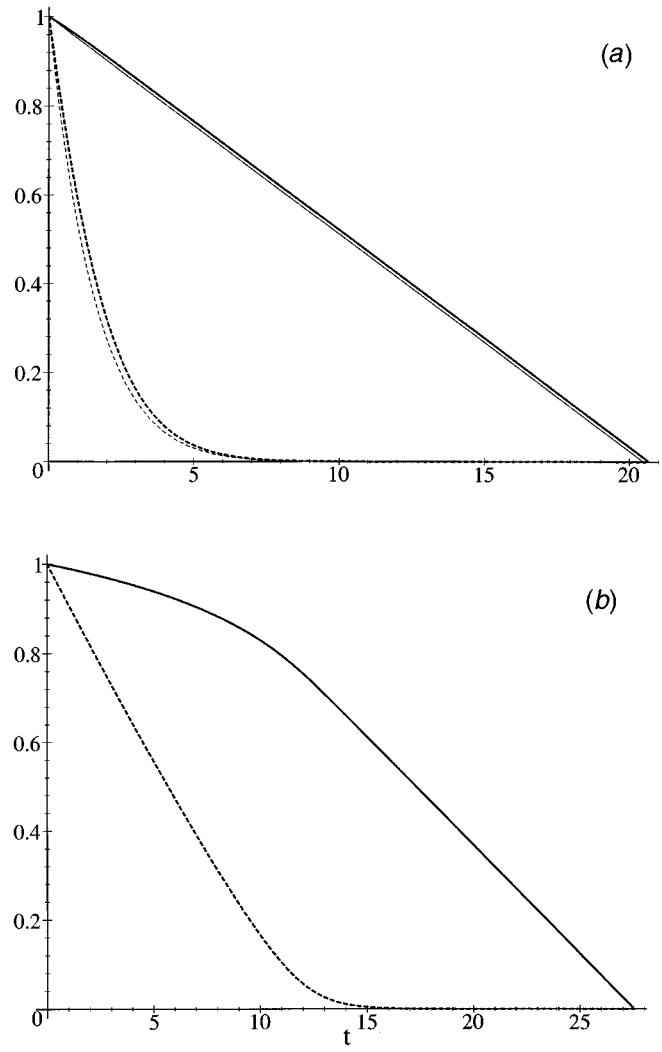

Fig. 2. Plots of $\omega(t)/\omega_0$ (solid curve) and $v(t)/v_0$ (dashed curve) as functions of time t (in seconds) for $\epsilon = 0{\cdot}1$ for the following values of the ratio $s_0 \equiv v_0/r\omega_0$: (*a*) $s_0 = 0{\cdot}1$, with the initial speed $v_0 = 0{\cdot}1$ $\mathrm{m\,s^{-1}}$, and the initial angular speed $\omega_0 = 16$ $\mathrm{s^{-1}}$; (*b*) $s_0 = 1$, with $v_0 = 1$ $\mathrm{m\,s^{-1}}$, and $\omega_0 = 16$ $\mathrm{s^{-1}}$. In both cases we have $\mu = 0{\cdot}0125$. Note the agreement between the analytical curves (lighter lines) and numerical curves (heavier lines) in part (*a*).

In these figures we see that the time t_{rot} taken for rotational motion to cease exceeds the time t_{trans} taken for translational motion to cease, especially for

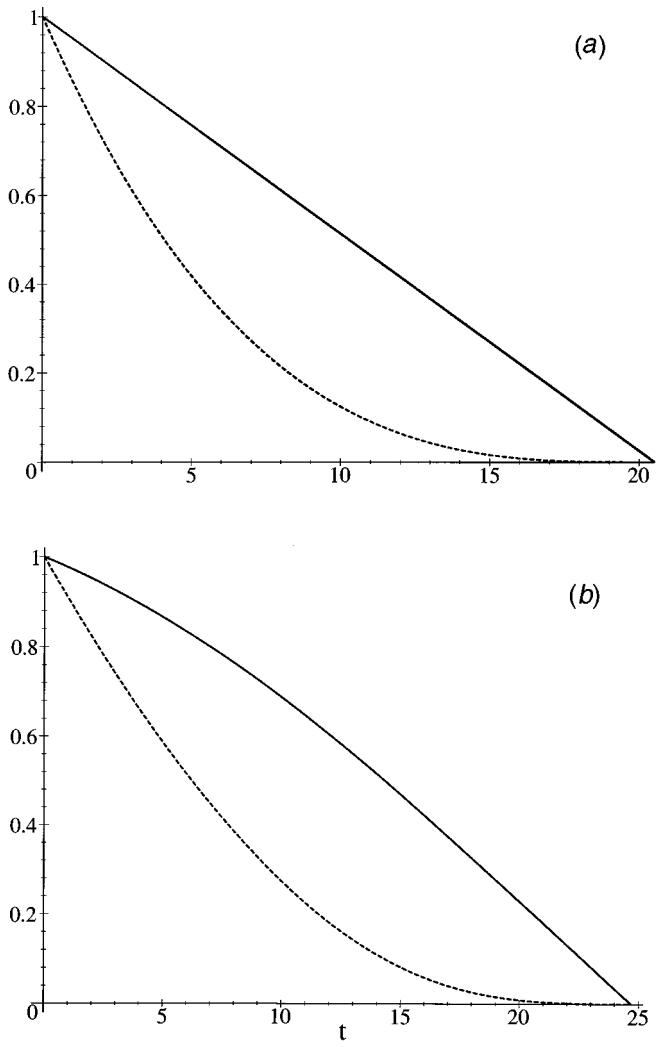

Fig. 3. As in Fig. 2, but with $\epsilon = 0{\cdot}4$.

small ϵ (Fig. 2). For example, in Fig. 2*a*, with $\epsilon = 0{\cdot}1$ and $s_0 = 0{\cdot}1$, we have $t_{trans} < 7$ s, while $t_{rot} \approx 20{\cdot}5$ s. We find that $t_{trans} < t_{rot}$ in all cases where $0 < \epsilon < 1$. In such cases, the motion is purely rotational for $t_{trans} < t < t_{rot}$. We also find that $t_{trans} = t_{rot}$ for $\epsilon = 1$.

In the $\epsilon = 1$ case, we are dealing with motions of cylinders over surfaces for which there is little or no melting, and thus the forces exerted on the contact areas are opposite to the directions of motion *relative to the surface*. That $t_{trans} = t_{rot}$ for such cases is observed in numerous examples, such as rotation and sliding of an overturned glass on a smooth surface, or for the motion of a hockey puck on flat ice (Voyenli and Eriksen 1985, 1986). We also find $t_{trans} \approx t_{rot}$ when $\epsilon \approx 1$, as is the case for curling rocks when $r\omega_0 < < v_0$ (slow rotation); this applies for almost all shots made by competent, experienced curlers. We further note

that the ratio t_{trans}/t_{rot} increases with increasing ϵ, and differs significantly from unity only for somewhat small values of ϵ.

In Fig. 4, where $s_0 = 20$ and $\epsilon = 1$, we have the motion corresponding to a slowly rotating curling shot, namely one where the rock travels down the ice and stops after traveling a total distance of about 29 m. Since $\epsilon = 1$, we see that translational and rotational motion cease at the same instant ($t_{trans} = t_{rot}$). (We point out that $s_0 \approx 20$ corresponds to a typical value for most slowly rotating curling rock shots.)

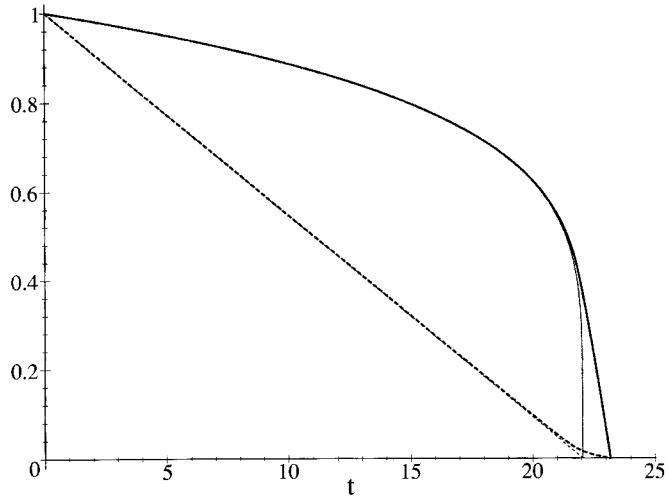

Fig. 4. Plots of $\omega(t)/\omega_0$ (solid curve) and $v(t)/v_0$ (dashed curve) as functions of time t (in seconds) for $\epsilon = 1$ and $s_0 = 20$; $v_0 = 2{\cdot}7$ $\mathrm{m\,s^{-1}}$, and $\omega_0 = 2{\cdot}16$ $\mathrm{s^{-1}}$. The analytical curves (lighter lines) and numerical curves (heavier lines) deviate just before motion ceases, and are in excellent agreement otherwise.

Upon examining all of the curves in Figs. 2–4 collectively, some notable features are evident. Perhaps most striking is the excellent agreement between the (exact) numerical results and the approximate, asymptotic analytical forms. Consider first part (a) in Figs 2 and 3. The analytical and numerical curves are almost indistinguishable in Fig. 3a, and are very close even in Fig. 2a. Such good agreement is surprising, especially upon realising that the value of the 'small' expansion parameter, $v(t)/\epsilon r\omega(t) \equiv s(t)/\epsilon$ has, initially, the value $s_0/\epsilon = 1$ in Fig. 2a and $s_0/\epsilon = 0{\cdot}25$ in Fig. 3a. Consider next Fig. 4. The analytical and numerical curves are almost indistinguishable except for the final second or so of the motion. The deviation between numerical and analytical curves near the end of the motion is expected, because the expansion parameter, $r\omega(t)/v(t)$, becomes arbitrarily large as $v(t) \to 0$. Consequently, the numerical and analytical curves *must* deviate just before motion ceases. The stopping time given by equation (10) is a good approximation, but is not the same as that given by the numerical curves.

Another interesting feature is that $\omega(t)$ is very nearly linear in t in part (a) of Figs 2 and 3, while $v(t)$ is very nearly linear in Fig. 4. If one generates the

curves of Fig. 4 changing only the value of ϵ, one finds very little change, even for ϵ as small as $0{\cdot}1$. Figs 2–4 collectively give a comprehensive picture of the motion as it depends upon ϵ and μ.

Before comparing our model with observed motions, we note that it is important to be aware of a key aspect of the cessation of translational motion. Recall that curling ice is not perfectly flat: it is pebbled, having rounded protrusions and accompanying valleys. Consequently, as the rock moves over the ice, its centre of mass will experience small changes in its vertical position, and thus also in its gravitational potential energy. There is a minimum translational speed which the rock must have if the leading edge of the rock is to be able to rise a vertical distance h_{peb} higher than the trailing edge. A simple calculation shows that the minimum speed is given by $v_{min} \approx (gh_{peb})^{\frac{1}{2}}$. For example, if $h_{peb} \approx 0{\cdot}01$ mm, then $v_{min} \approx 1$ cm s^{-1}. The value of v_{min} will depend on the nature of the pebbled ice. In one observed motion we found $v_{min} \approx 4$ cm s^{-1} (see Fig. 5 below). Note that h_{peb} is the scale over which the vertical position of the rock's centre of mass varies, and is *not* the size of the pebbles themselves. The important consequence of this minimum speed is that real curling rocks will stop somewhat suddenly, albeit at a rather slow speed.

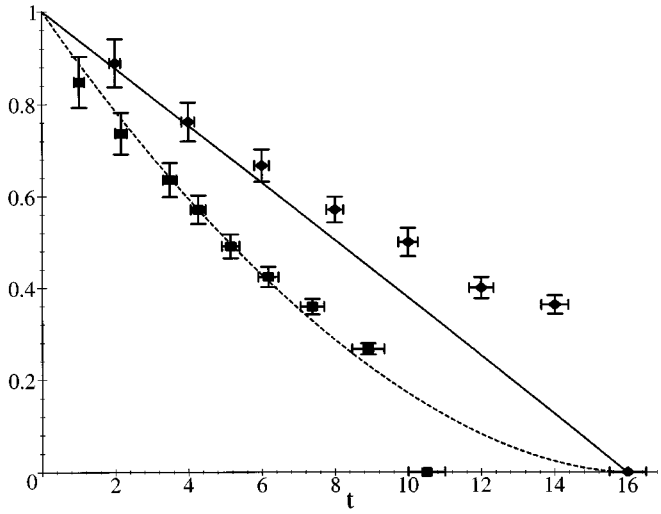

Fig. 5. Calculated curves for $\omega(t)/\omega_0$ (solid curve) and $v(t)/v_0$ (dashed curve) as functions of time t (in seconds) for comparison with the actual motion of a rapidly rotating curling rock. Observed values of $\omega(t)/\omega_0$ (diamonds) and $v(t)/v_0$ (squares) are also shown. The observed values of v_0 and ω_0 are $v_0 = 0{\cdot}22$ m s^{-1} and $\omega_0 = 11{\cdot}8$ s^{-1}. Values for ϵ and μ were estimated from the observed stopping time for rotational motion along with equations (7) and (8): we estimated $\epsilon = 0{\cdot}7$ and $\mu = 0{\cdot}012$.

In Fig. 5 we compare our model with the observed motion of a rapidly rotating curling rock. The shot for Fig. 5 was a short shot, traveling a total distance $y_{tot} \approx 1{\cdot}6$ m, with translational motion ceasing after about 10 s, while rotational motion ensued for a total of about 16 s. The theoretical curves are

in qualitative agreement with the observed data. There is good quantitative agreement as well. The theoretical curves for both $v(t)/v_0$ and $\omega(t)/\omega_0$ agree with the data for $0 < t \lesssim t_{trans} \approx 10$ s. As anticipated, $v(t)$ drops quickly to zero once $v(t) \approx v_{min}$; from Fig. 5, we estimate $v_{min} \approx 4$ cm s^{-1}. The observed values of $\omega(t)$ are not linear for $t_{trans} < t < t_{rot}$. One possible explanation is that μ for purely rotational motion could be smaller than for translational motion. This is in accord with our expectation that ϵ and μ could have complicated time-dependencies. There are of course other possibilities; further work will be needed to examine this part of the motion.

From Fig. 5 we also see that $\omega(t)$ drops rapidly to zero once $\omega(t) \approx \omega_{min}$; this could have been predicted on the basis of the following physical argument. The contact annulus must have some minimum speed to induce kinetic melting. Once ω drops to a small enough value, the liquid film can no longer be sustained and thus freezes, with rotational motion ceasing almost immediately thereafter.

The data for Fig. 5 were obtained by videotaping the short shot, with the rock moving parallel to a distance indicator, and with the camera far enough away (approximately 20 m) that the error with changing angle was negligible. The translational and rotational speeds were obtained by simply counting frames to determine the time elapsed to move a given distance or to execute half a rotation. The dominant sources of error were thus the time lag (1/60 s) between successive frames and the time intervals over which the speeds were measured.

In Table 1 we compare our model with other observed motions of rapidly rotating curling rocks. The values of v_0 and ω_0 given are observed values. The results are arranged in order of increasing v_0 and also increasing $s_0 \equiv v_0/r\omega_0$.

Table 1. Observed and calculated quantities for rapidly rotating curling rocks

Shown are the initial speed v_0, initial angular speed ω_0, the ratio $s_0 \equiv v_0/(r\omega_0)$, and ϵ for three distinct shots. The observed and calculated values of the duration of translational motion, t_{trans}^{obs} and t_{trans}^{calc}, the duration of rotational motion, t_{rot}^{obs} and t_{rot}^{calc}, and the total distance traveled, y_{tot}^{obs} and y_{tot}^{calc}, are also compared. The effective coefficient of kinetic friction μ is 0·0125 in all cases

Shot	Short	Medium	Long
v_0 (m s^{-1})	0·28	0·84	2·4
ω_0 (s^{-1})	19·8	19·8	11·1
s_0	0·23	0·68	3·46
ϵ	0·2	0·4	0·5
t_{trans}^{obs} (s)	10	19	25
t_{trans}^{calc} (s)	11	22	26
t_{rot}^{obs} (s)	26	26	27
t_{rot}^{calc} (s)	26	28	29
y_{tot}^{obs} (m)	1·2	8·2	30
y_{tot}^{calc} (m)	1·1	6·5	27

The values used for ϵ were selected using the insight gained from Figs 2 and 3. For example, for the short shot, the total distance traveled was $y_{tot} \approx 1{\cdot}2$ m, with translational motion ceasing after about 10 s, while rotational motion ensued for a total of about 26 s. Assuming a small value for v_{min}, we see from Figs 2 and 3 that this motion corresponds to small ϵ, and we chose $\epsilon = 0{\cdot}2$ for the short shot in Table 1. Having chosen ϵ, we are at liberty to adjust slightly

the value of μ from its original value of $0{\cdot}0125$. It turns out, however, that the value $\mu = 0{\cdot}0125$ gives the best agreement with observed values for the choices of ϵ.

In the second entry in Table 1, the shot traveled a distance $y_{tot} \approx 8$ m. Translational motion lasted for about 19 s, rotational motion about 26 s. Again, from Figs 2 and 3, we see that an appropriate choice is $\epsilon = 0{\cdot}4$.

In the final entry, the shot traveled a distance $y_{tot} \approx 30$ m. Translational motion lasted for about 25 s, rotational motion about 27 s. We take $\epsilon = 0{\cdot}5$ for the numerical run. Note also that we have $v_0 \approx 3{\cdot}5r\omega_0$, so we do not expect much difference between t_{trans} and t_{rot}, even though this shot has a much greater rotational speed than shots commonly made by competent curlers.

The observed and calculated values of various physical quantities, such as t_{trans} and t_{rot}, are also compared in Table 1. In examining Table 1, recall that t_{trans} is given by $v(t_{trans}) \approx 1$ cm s^{-1}. (Note that the shots in Table 1 were made on a different sheet of ice than the sheet for the shot in Fig. 5.) The observed values and the values obtained from our model are in good agreement. This agreement supports our decision to use constant, effective values for μ and ϵ, as discussed earlier.

5. Discussion and Conclusion

We conclude that the essential ideas in this manuscript are viable candidates for the explanation of the motion of a rapidly rotating curling rock. We emphasise that the results for $v(t)$ and $\omega(t)$ in our model simulations exhibit the correct *qualitative* motion as well as good *quantitative* results. More work is required to fully understand and explain the purely rotational phase of the motion.

Rapidly rotating curling rocks are observed to stop moving translationally long before they stop rotating; our model successfully accounts for this rather novel feature of the motion of curling rocks. We emphasise that our idea of the existence of the liquid film and its tendency to be drawn around the rock is crucial for explaining the phenomenon of translational motion ceasing prior to rotational motion.

We point out that other models appear to be unable to explain the motion of rapidly rotating curling rocks. One example is a model proposing that the lateral motion of slowly rotating curling rocks results as a consequence of the nonuniform pressure distribution around the contact annulus, the leading semi-circle being subjected to a higher pressure than the trailing semi-circle in order to counteract the lateral torque caused by friction (Johnston 1981). It was argued that the higher leading pressure results in lower friction. In this model, the frictional force exerted on any portion of the rock is opposite in direction to the velocity relative to the ice, which thus requires the translational and rotational motions to stop at the same time, contrary to what is actually observed. Another paper by Denny (1998) considered a 'left–right' asymmetry. We have carefully examined the approach taken in that publication, and have found that there are serious inadequacies in the approach. The biggest problem with the approach is the following. It predicts that two curling rocks, released at different times and from different initial locations, but such that they are moving in the same direction and with the same speed at a later time (i.e. are moving 'side by side') will, subsequently, follow different trajectories, and upon stopping can have a lateral

separation by as much as $0{\cdot}4$ m. This is clearly physically unreasonable, and is in severe disagreement with observed motions of slowly rotating curling rocks. Our findings are reported in Shegelski and Reid (1999). Since this approach (Denny 1998) fails to explain why a slowly rotating curling rock curls, it is not appropriate to consider it for the case of rapidly rotating curling rocks.

The work in this paper and that presented in our previous paper (Shegelski *et al*. 1996) combine to account both qualitatively and quantitatively for several aspects of the observed motions of real curling rocks, both slowly rotating and rapidly rotating. Some of the successes of our model are as follows.

Slowly rotating curling rocks. Our model accounts for the following: (1) why curling rocks curl; (2) the direction and amount of curl; (3) the time taken to go from hog line to hog line; (4) the time taken to go from hog line to tee line; and (5) the total number of rotations of the rock from release to stopping.

Rapidly rotating curling rocks. In this paper we have shown that our model further explains the following: (6) that translational motion ceases prior to rotational motion; (7) the nature of the time-dependencies of $v(t)$ and $\omega(t)$; and (8) the total distance travelled. Other successes of the model are noted in Shegelski *et al*. (1996).

In view of these agreements between the observed motions of curling rocks and the motions given by our model, we conclude that our model presents a reasonable picture of the underlying physics of the motions of curling rocks.

Acknowledgments

We thank the Prince George Golf and Curling Club (PGGCC) for the use of their facilities, and we thank Murry Kutyn (Head Ice Technician at PGGCC) for useful information. We also thank the Educational and Media Services of UNBC, especially Mr Andrew Zand, for use of equipment. We thank Matthew Reid for assistance with some aspects of this work. We thank the referees for constructive comments. This work was partially supported by the Natural Sciences and Engineering Research Council of Canada.

References

Canadian Curling Association, 'The Rules of Curling' (Canadian Curling Association: Gloucester, Ontario).
Denny, M. (1998). *Can. J. Phys.* **76**, 295.
Johnston, G. W. (1981). *Can. Aeronautics Space J.* **27**, 144.
Shegelski, M. R. A., and Reid, M. E. (1999). *Can. J. Phys.*, submitted.
Shegelski, M. R. A., Niebergall, R., and Walton, M. A. (1996). *Can. J. Phys.* **74**, 663.
Shegelski, M. R. A., Niebergall, R., and Walton, M. A. (1997). *Phys. World* **10(6)**, 19.
Voyenli, K., and Eriksen, E. (1985). *Am. J. Phys.* **53**, 1149.
Voyenli, K., and Eriksen, E. (1986). *Am. J. Phys.* **54**, 778.

Manuscript received 2 September 1998, accepted 17 June 1999